Biomech Model Mechanobiol (2010) 9:163–175
DOI 10.1007/s10237-009-0167-0

ORIGINAL PAPER

# Proposed role of the M-band in sarcomere mechanics and mechano-sensing: a model study

**A. A. Shabarchin · Andrey K. Tsaturyan**

Received: 22 November 2008 / Accepted: 22 July 2009 / Published online: 8 August 2009


**Abstract** In sarcomeres of striated muscles the middle parts of adjacent thick filaments are connected to each other by the M-band proteins. To understand the role of the M-band in sarcomere mechanics a model of forces which pull a thick filament to opposite Z-disks of a sarcomere is considered. Forces of actin-myosin cross-bridges, I-band titin segments and the M-band are accounted for. A continual expression for the M-band force is obtained assuming that the M-band proteins which connect neighbor thick filaments have nonlinear elastic properties. On the ascending and descending limbs of the force-length diagram cross-bridge forces tend to destabilize sarcomere while titin tries to restore its symmetric configuration. When destabilizing cross-bridge force exceeds a critical limit, symmetric configuration of a sarcomere becomes unstable and the M-band buckles. Stiffness of the M-band increases stability only if the M-band is anchored to the extra-sarcomere cytoskeleton. Realistic magnitudes of the M-band buckling require that the M-band proteins have essentially nonlinear elasticity. The buckling may explain the M-band bending and axial misalignment of the thick filaments observed in contracting muscle. We hypothesize that the buckling stretches the titin protein kinase domain localized in the M-band being the signal for mechanical control of gene expression and protein turnover in striated muscle.

**Keywords** Striated muscle · Sarcomere · Cross-bridges · Titin · M-band · Stability

A. A. Shabarchin · A. K. Tsaturyan (✉)
Department of Biomechanics, Institute of Mechanics,
M.V. Lomonosov Moscow University, 1 Mitchurinsky prosp.,
119992 Moscow, Russia
e-mail: tsat@imec.msu.ru

## 1 Introduction

In striated muscles the middle parts of adjacent thick filaments in sarcomeres are tied to each other in the M-band (Luther and Squire 1978). Together with the I-band titin segments which connect the tips of the thick filaments to the Z-disks, the M-band proteins keep the thick filaments in the middle of sarcomere providing optimal performance (Agarkova and Perriard 2005). The M-band was assumed to be a "safeguard of sarcomere stability" (Agarkova et al. 2003) although its mechanical function was not studied either experimentally or theoretically. Several proteins including myomesin-1, M-protein or myomesin-2 (Grove et al. 1984), myomesin-3 (Schoenauer et al. 2008), obscurin (Fukuzawa et al. 2008), muscle-type creatine kinase (MM-CK, Hornemann et al. 2003) and the C-terminal fragment of titin (Obermann et al. 1996) have been localized in the M-band. Mechanical properties of some of these proteins were studied using atomic force microscopy (Schoenauer et al. 2005; Puchner et al. 2008). Obscurin was shown to participate in connection between the M-band myomesin (Fukuzawa et al. 2008) and extra-sarcomere protein ancyrin-B located in sarcolemma (Cunha and Mohler 2008). Obscurin was also found across the whole structure that connects the M-bands of sarcomeres in neighbor myofibrils (Carlsson et al. 2008). The M-band fragment of titin contains a protein kinase domain (TK) that was recognized as mechano-sensor that controls the dependence of gene expression and protein turnover on mechanical state of muscle (Lange et al. 2005). Stretch of TK by ca. 9 nm promotes its enzymatic activity (Puchner et al. 2008). It however remains unclear how TK may sense mechanical state of life muscle. If all thick filaments in a sarcomere stay exactly in the middle of sarcomere and the M-band remains flat then tension developed by myosin

cross-bridges should not induce any stretch of TK domain that is needed for its activation.

There are two lines of evidences showing the presence of substantial shear strain in the M-band upon development of active force. Bending of the M-bands during contraction of muscle fibers with permeabilized cell membrane was observed by electron microscopy (Horowits and Podolsky 1987). Widening of the M3 meridional myosin reflection on the x-ray diffraction pattern during force development results from a substantial axial misalignment of the thick filaments (Huxley et al. 1982). The width of the M3 reflection in the equatorial direction is reciprocal to the lateral width of the bunch of coherently scattering thick filaments. When the filaments are misaligned due to a shear strain in the M-band the M3 widens. The shear strain within the M-band upon muscle contraction was assumed to trigger TK activation (Puchner et al. 2008). It however remains unclear how and why the M-band bends when myosin cross-bridges produce high force and what is the particular mechanical signal that induces the shear strain of the M-band and stretch of TK.

A question that is discussed for more than 50 years (Hill 1953) is sarcomere stability. The presence of a negative slope region on the relationship between net tension and a half-sarcomere length suggests that symmetric configuration of a sarcomere should be unstable (Zahalak 1997). Moreover, symmetric configuration of a sarcomere can be unstable not only on the descending limb of the force-length relationship, but also on its ascending limb if the resultant cross-bridge force which pulls a thick filament to one of the Z-disks prevails over the net titin force which keeps the filament in the middle of the sarcomere. Indeed the movement of the A-band towards a Z-disk was observed after long-term isometric contractions of chemically skinned rabbit muscle fibers (Horowits and Podolsky 1987) and in the experiments with single isolated myofibrils (Telley et al. 2006). In both cases the connections between the M-band and extra-sarcomere cytoskeleton are probably damaged or at least weaken. Under less severe conditions the M-band in muscle fibers does not move to a Z-disk, but bends in such way that its deviation from the middle plane of sarcomere is minimal at the sarcomere boundary and maximal in its center (Horowits and Podolsky 1987). The reason for the M-band bending and the role of the M-band in stability of symmetric configuration of a sarcomere during muscle contraction remain unclear.

To address these questions we suggest a model of thick filament mechanics in sarcomeres of striated muscle. The model takes into account forces of cross-bridges, I-band regions of titin. For the M-band proteins we use a continual description of the elastic forces between neighbor thick filaments packed to a hexagonal lattice. Also elastic connections between the M-bands on the boundary of a sarcomere and extra-sarcomere cytoskeleton are accounted for. The model suggests that symmetric configuration with flat M-band in the middle of sarcomere is stable only if the cross-bridge force remains below a critical limit. At super-critical tension the M-band buckles and bends. The buckling amplitude is limited mainly by nonlinear elasticity of the M-band proteins which in this case protect sarcomere from damage by high load. We also hypothesize that the M-band buckling under super-critical load triggers TK activation being the signal that controls mechano-sensing of gene expression and protein turnover.

## 2 Model

### 2.1 Notations

$u$: axial displacement of a thick filament from the middle of a sarcomere;
$v = \partial u/\partial t$ : sliding velocity of a thick filament (time derivative of $u$);
$l_p = 1.2$ nm:persistence length of the I-band titin segment (Leake et al. 2004);
$l_c = 1.15$ μm: contour length of the same titin segment (Leake et al. 2004);
$l$: half-sarcomere length;
$l_m = 0.82$ μm: half-length of a myosin filament (Sosa et al. 1994);
$l_a = 1.12$ μm: length of an actin filament (Sosa et al. 1994);
$l_b = 0.08$ μm: half-length of the "bare zone" in the middle of a thick filament;
$f_{tL,R}$: force of the I-band titin segments for the left (L) or right (R) tips of a thick filament;
$f_{xbL,R}$: cross-bridge forces for the left (L) or right (R) halves of a thick filament;
$w_{L,R}$: lengths of overlap zones in the left (L) and right (R) halves of a thick filament;
$f_0$: isometric cross-bridge force per length of the overlap zone;
$\beta$: effective viscosity of cross-bridges;
$f_M$, $f_{Mi}$: resulting M-band force of a thick filament and force between a thick filament and its $i$-th neighbor;
$d$: distance between neighbor thick filaments;
$k$: shear stiffness of the M-band bond between neighbor thick filaments;
$m$: non-linearity parameter for the same stiffness.
$E$: stiffness of the extra-sarcomere structures holding a boundary thick filament in the middle of sarcomere.

### 2.2 Force balance

We consider mechanics of a single thick filament in a sarcomere. Figure 1 schematically shows mechanical components of a sarcomere and forces of the cross-bridges, I-band titin segments and the M-band proteins which pull a thick

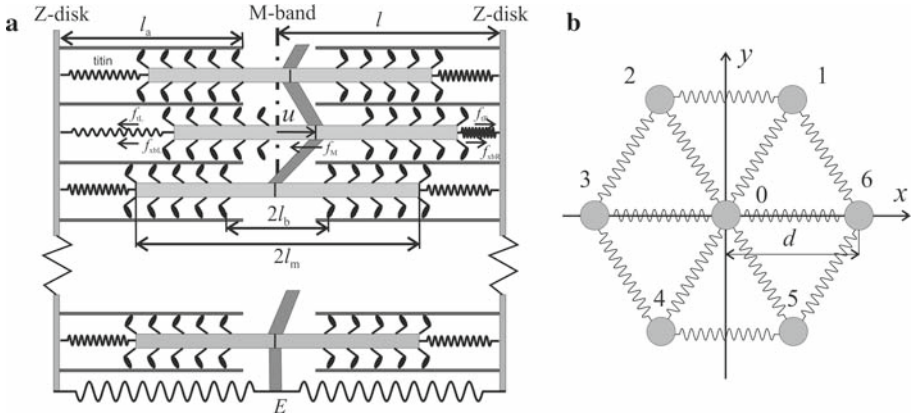


**Fig. 1** Schematic representation of thick filament mechanics in the model. **a** Longitudinal section. Thin (*dark gray*) and thick (*light gray*) filaments and cross-bridges (*black*) are shown. Displacement of the center of a thick filament from the middle of sarcomere is $u$. Springs which connect the Z-disk to the tips of the thick filaments represent the I-band titin segments. Titin and cross-bridge forces pulling a thick filament towards the left (L) and right (R) Z-disks are shown by arrows. Gray parallelograms between the thick filaments represent the M-band proteins which resist shear strain with force $f_M$. A thick filament on the boundary of the M-band is shown at the bottom of the figure. It is connected not only to neighbor thick filaments, but also to extra-sarcomere cytoskeleton shown as two springs which connects its M-band segment to both Z-disks with effective stiffness $E$ each. Half length of a sarcomere, $l$, of a thick filament, $l_m$, and of its bare zone, $l_b$, and length of a thin filament, $l_a$. Forces are labeled as in Eq. 1. **b** Transversal section. Seven thick filaments in hexagonal lattice are shown as gray circles. Springs between them represent the M-band proteins. Coordinate system $x$, $y$ has its origin in the center of 0th filament, its 6 neighbors are labeled with $i = 1, \ldots, 6$

filament. For simplicity both Z-disks and the thin (actin) filaments are assumed to stay immobile while the thick filaments are able to slide along their axes towards one of the Z-disks. We neglect compliance of the thin and thick filaments as changes in their lengths are within a few nanometers (Huxley et al. 1994; Wakabayashi et al. 1994), a value that is much smaller than axial displacement of the thick filaments from the middle of the sarcomere considered here. For the same reason elongation of the thin filaments due to binding of myosin heads (Tsaturyan et al. 2005) was also neglected. As inertial forces are small and therefore can be omitted the force balance equation taking into account titin, cross-bridge and M-band forces (Fig. 1a) can be written as

$$f_{tR} - f_{tL} + f_{xbR} - f_{xbL} + f_M = 0 \tag{1}$$

where $f_{tR}$, $f_{tL}$ are the I-band titin forces and $f_{xbR}$, $f_{xbL}$ are the cross-bridge forces which pull the filament toward the right (R) and left (L) Z-disk of the sarcomere, respectively; $f_M$ is the shear force of the M-band proteins which connect the thick filament to its neighbors.

### 2.3 Titin force

We assumed titin to be purely elastic and expressed its elasticity using a worm-like chain approximation (Leake et al. 2004)

$$f_{tit}(\lambda) = \frac{6k_BT}{L_p}\left(\frac{1}{4\,(1-\lambda/L_c)^2} + \frac{\lambda}{L_c} - \frac{1}{4}\right) \tag{2}$$

where $\lambda$ is the distance between the tip of the thick filament and the Z-disk, $L_p$ and $L_c$ are constants called persistence length and contour lengths, respectively; $k_B$ and $T$ are the Boltzmann constant and absolute temperature. Factor of 6 represents 6 titin molecules connecting the filament to each Z-disk (Liversage et al. 2001). Therefore the net titin forces in Eq. 1 can be expressed as

$$F(u) = f_{tR} - f_{tL} = f_{tit}\,(l - l_m - u) - f_{tit}\,(l - l_m + u) \tag{3}$$

where $u$ is the axial displacement of the filament from the middle of the sarcomere, $l$ and $l_m$ are half-sarcomere length and half-length of a thick filament (Fig. 1a) and function $f_{tit}$ is determined by Eq. 2.

### 2.4 Cross-bridge forces

The cross-bridge forces in Eq. 1 are proportional to the length of the overlap zone between the thin filaments and the myosin head region in the right, $w_R$, and left, $w_L$, halves of a thick filament and to the average force produced by cross-bridge per unit length of the overlap zone. We assume that the cross-bridge forces can be expressed as

$$f_{xbR} = w_R f_0\,(1 - p(v))\,, \quad f_{xbL} = w_L f_0\,(1 - p(-v))$$

where $f_0$ is the linear density of isometric cross-bridge force (force per length of the overlap zone) and $v = \partial u/\partial t$ is the filament sliding velocity. Function $p(v)$ describes the Hill force–velocity relation; $p$ is zero during isometric

contraction, i.e. at zero velocity ($p(0) = 0$) and equals to 1 at maximal shortening velocity, $v_{\max}$: $p(v_{\max}) = 1$. For simplicity we will use a linear approximation of the Hill equation assuming that $p(v) = \beta v$ where $\beta$ is a constant that is of order of magnitude of $1/v_{\max}$. With the above assumption, the total cross-bridge force can be expressed as

$$f_{xb} = -\beta f_0 v \left[w_R(u) + w_L(u)\right] + f_0 \left[w_R(u) - w_L(u)\right]. \tag{4}$$

Due to axial symmetry $w_L(u) = w_R(-u)$. The overlap lengths on the right and left halves of a thick filament, $w_R$ and $w_L$, depend not only on the filament displacement, $u$, but also on the half-sarcomere length, $l$. On the descending limb of the length-force relationship, i.e. at $l > l_a + l_b$, $w_R(u)$ can be expressed as

$$w_R(u) = \begin{cases} u + l_m + l_a + l_b - l, & l - l_a - l_b > u > l_a + l_b - l; \\ l_m - l_b, & u > l - l_b - l_a. \end{cases} \tag{5}$$

Here $2l_b$ is the length of the bare zone without cross-bridges in the middle of a thick filament (Fig. 1a). The overlap difference $w_R(u) - w_L(u) = 2u$ for $|u| < l - l_a - l_b$. Outside this range it also increases linearly with $u$, but the slope decreases from 2 to 1.

On the plateau of the force-length relationship, where $l_a - l_b < l < l_a + l_b$, there is a 'neutral region' of small displacement, $|u| < l_b + l_a - l$, where $w_R$ and $w_L$ remain constant, equal to maximal overlap length per a half of a thick filament ($w_R = w_L = l_m - l_b$). Outside the 'neutral region' $w_R - w_L$ increases linearly with $u$ with slope 1.

On the ascending limb where $l < l_a - l_b$ the thin filaments from two halves form a double-overlap zone that overlaps with the myosin head region of the thick filaments. In this double overlap zone myosin heads cannot properly interact with normally oriented actin filaments and do not produce active force (Trombitás and Tigyi-Sebes 1984). From mechanical point of view this is equivalent to the reduction of the length of the thin filaments from $l_a$ to $2l - l_a$. Thus

$$w_R = \begin{cases} u + l_m - l + l_a, & l - l_a - l_b < u < l_a + l_b - l; \\ l_m - l_b, & u > l_a + l_b - l. \end{cases} \tag{5'}$$

As in the case of the descending limb the difference between the lengths of the overlap zones $w_R(u) - w_L(u) = 2u$ for small $|u|$ and it increases linearly with $u$ with the slope of 1 at larger $|u|$. In all three cases, i.e. on the descending limb, the plateau, and the descending limb, $|u|$ is limited: $|u| < l - l_m$ because the thick filaments and the Z-disks are considered to be rigid.

Figure 2 shows the titin and cross-bridge forces as the function of the sarcomere length in the case when the M-band stays exactly in the middle of a sarcomere. The standard value

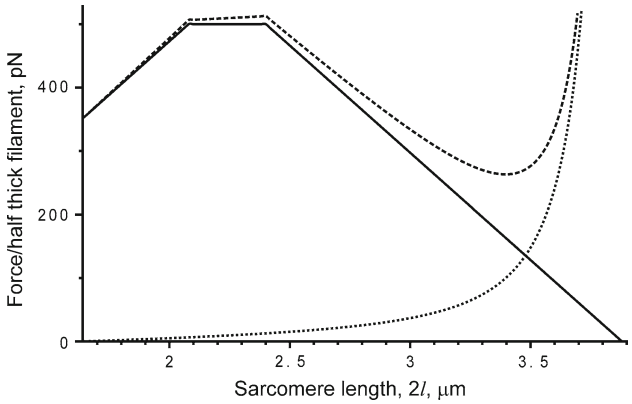


**Fig. 2** Model approximation of steady-state forces of cross-bridges (*continuous line*), I-band titin segments (*dotted line*) and of their sum (*dashed line*) as functions of sarcomere length, $2l$, in the case when the middle of the thick filament remains exactly in the middle of sarcomere

of isometric cross-bridge force per a half of a thick filament on the plateau of the length-force relationship at full activation, $F_0$, was set to 500 pN, or 1.6 pN per a myosin head. As not all myosin heads are attached to actin during muscle contraction average force produced by an attached head is probably at least twice higher. This estimate corresponds to $f_0 = F_0/(l_m - l_b) = 500/(l_m - l_b) = 675$ pN/μm that gives sarcomere tension of ca. 360 kN/m$^2$ if the distance between neighbor thick filaments, $d$, is 40 nm. Assuming that 80% of the cross-section area of a fiber is occupied by myofibrils this figure corresponds to fiber tension of 288 kN/m$^2$. The net force decreases in the beginning of the descending limb and increases at longer sarcomere length where the titin force prevails over the cross-bridge force (Fig. 2).

### 2.5 M-band force

We neglect viscoelastic properties of the M-band proteins and kinetics of protein folding–unfolding (Schoenauer et al. 2005; Puchner et al. 2008) and assume that the M-band force is purely elastic. The shear force between two adjacent thick filaments depends on the shear strain or in other words on the difference, $u_i - u_0$, of the displacements of the two neighbor filaments from the middle of sarcomere (one filament is labeled as 0th, another filament as $i$th). Due to symmetry the direction of the force should revert when $\Delta u$ changes its sign. Therefore it should be an odd function of $u_i - u_0$. We will approximate the force by a third order polynomial keeping only the linear and the main non-linear (third order) terms:

$$f_{Mi} = k\left(u_i - u_0 + m\left(u_i - u_0\right)^3\right) \tag{6}$$

where $k$ and $m$ are stiffness and non-linearity parameter and $u_i - u_0$ is the difference in displacements of a 0th thick filament and its $i$th neighbor (Fig. 1b). The resulting M-band

force, $f_M$, is the sum of the M-band shear forces between the 0th central thick filament and its six neighbors in the hexagonal lattice (Fig. 1b), i.e.

$$f_M = \sum_{i=1}^{6} f_{Mi}, \quad i = 1, \ldots, 6. \tag{7}$$

To obtain closed expression of $f_M$ we introduce Cartesian coordinates with $x$ and $y$ axes perpendicular to the filament axis and $z$ parallel to it. The origin is on the axis of a thick filament (called 0th filament) and $z = 0$ in the middle of the sarcomere (Fig. 1b). Although $u$ is determined only in discrete points where the thick filaments are located, one can define a smooth function $u(x, y)$ that coincides with axial displacement of each thick filament in a sarcomere in the point of their localization. We also assume that the distance, $d$, between neighbor thick filaments remains constant. To calculate the M-band force $f_M$ we firstly expand $u$ to a Taylor series assuming that it is twice differentiable

$$u(x, y) = u(0, 0) + \frac{\partial u(0, 0)}{\partial x} x + \frac{\partial u(0, 0)}{\partial y} y + \frac{\partial^2 u(0, 0)}{\partial x^2} \frac{x^2}{2} + \frac{\partial^2 u(0, 0)}{\partial y^2} \frac{y^2}{2} + \frac{\partial^2 u(0, 0)}{\partial x \partial y} xy + \cdots \tag{8}$$

Then we specify the coordinates, $x_i$, $y_i$, of the $i$th neighbor filament in the hexagonal lattice using expressions

$$x_i = d \cos\left(\frac{\pi i}{3}\right), \quad y_i = d \sin\left(\frac{\pi i}{3}\right)$$

where $d \approx 40$ nm is the distance between neighboring myosin filaments (Fig. 1b). On the next step for each neighbor filament we specify $x_i$, $y_i$ in Eq. 8 and calculate its displacement, $u_i = u(x_i, y_i)$, and the difference, $u_i - u_0$, in displacements of the $i$th and 0th filaments, where $u_0 = u(0,0)$. Using the obtained expressions for $u_i - u_0$ the M-band force between the 0th myosin filament and one of its neighbors, $f_{Mi}$, can be calculated using Eq. 6. Then after summation of all 6 forces which pull the 0th myosin filament (Eq. 7) the M-band force can be obtained of the form

$$f_M = \sum_{i=1}^{6} f_i = \frac{3kd^2}{2} \mathrm{div}\left\{\mathrm{grad}\left[u\left(1 + \frac{3md^2}{4}(\mathrm{grad}u)^2\right)\right]\right\} + o(d/L)^3$$

or

$$f_M \approx \frac{3kd^2}{2}\left\{\Delta u + \frac{3md^2}{4}\mathrm{div}\left[\mathrm{grad}u\,(\mathrm{grad}u)^2\right]\right\} \tag{9}$$

where div, grad and $\Delta$ are two-dimensional divergence, gradient and Laplace operators. As the sarcomere width, $L \approx 1$ μm and $d \approx 40$ nm, the dimensionless value $d/L$ can be considered as a small parameter $d/L \approx 0.04$. The first (linear) term of the M-band force is Laplacian. This means that for small displacement $u$ the M-band behaves like a thin elastic membrane. The last expression in Eq. 9 was obtained assuming that $md^2 \geq 1$ and neglecting all terms which are of order higher than $(d/L)^3$. The expression of the M-band force of the form Eq. 9 can be obtained for each filament in a sarcomere that is surrounded by six neighbor myosin filaments, i.e. for each internal thick filament. In other words Eq. 9 gives a continuum approximation of the M-band force inside a sarcomere. For the boundary thick filament the force balance gives a different expression that is considered in the next section.

Finally the equation that describes mechanics of the internal thick filaments in a sarcomere with fixed Z-disks can be obtained by substituting Eqs. 3, 4, 9 into the force balance Eq. 1. This gives

$$\beta\eta(u)\, f_0 v = \frac{3kd^2}{2}\left\{\Delta u + \frac{3md^2}{4}\mathrm{div}\left[\mathrm{grad}u\,(\mathrm{grad}u)^2\right]\right\} + \psi(u) \tag{10}$$

where functions $\eta(u) = w_R(u) + w_L(u)$; $\psi(u) = f_0(w_R(u) - w_L(u)) + F(u)$ describe the total overlap length for both halves of a thick filament and the total steady-state resultant force of cross-bridges and titin as function of displacement $u$.

### 2.6 Boundary conditions

The boundary conditions for Eq. 10 are determined by the connection between the M-band proteins and extra-sarcomere cytoskeleton and by the stiffness of the latter. The bond force balances the M-band force acting on a boundary thick filament from its neighbor thick filaments. Assuming that the extra-sarcomere structures connecting the Z-disks and the middle of a boundary thick filament can be described by a Hookean elastic elements with stiffness $E$ (Fig. 1a) the boundary conditions are of the form

$$\sqrt{3}kd\frac{\partial u}{\partial n} + 2Eu\Big|_{\Gamma} = 0 \tag{11}$$

where $\partial u/\partial n$ is the normal derivative of the thick filament displacement $u(x, y)$, and $n$ is the normal to the sarcomere boundary contour, $\Gamma$. If $E = 0$ the bond is loose and the M-band can move as a solid flat disk. If the bond is much stiffer than the M-band, then the M-band border remains fixed in the middle of sarcomere irrespectively to other forces (zero displacement condition).

## 3 Approximations of sarcomere cross-section

Cross-section shape of sarcomeres varies significantly. We therefore consider two extreme cases of its geometry: thin rectangular and round. In the first case, the cross-section is rectangular with one size (in the $y$ direction) much larger than the other size, $2R$ ($-R \leq x \leq R$). In the second case, the cross-section is a circle of radius $R$ ($0 \leq r \leq R$).

### 3.1 Dimensionless variables

We introduce dimensionless variables:

$$x' = \frac{x}{R}, \quad r' = \frac{r}{R}, \quad u' = \frac{u}{R}, \quad t' = \frac{3tkd^2}{4\beta F_0 R^2}.$$

Then omitting prime mark one can rewrite the force balance equation in dimensionless variables. For thin rectangular sarcomere Eq. 10 reduces to

$$\varsigma(u)\frac{\partial u}{\partial t} = \frac{\partial^2 u}{\partial x^2}\left(1+\mu\left(\frac{\partial u}{\partial x}\right)^2\right)+\varphi(u) \tag{12}$$

and the boundary conditions Eq. 11 are of the form

$$\begin{aligned}&\alpha\cdot\partial u/\partial x - u = 0 \quad \text{at } x=-1,\\ &\alpha\cdot\partial u/\partial x + u = 0 \quad \text{at } x=1,\end{aligned} \tag{12'}$$

where dimensionless parameters $\mu$, $\alpha$; the normalized overlap, $\zeta(u)$, and the net 'elastic' force, $\varphi(u)$, functions are

$$\mu = \frac{9md^2}{4}, \quad \alpha = \frac{\sqrt{3}kd}{2ER}, \quad \varsigma(u) = \frac{w_R(uR)+w_L(uR)}{2(l_m-l_b)},$$

$$\varphi(u) = \frac{2R^2\psi(uR)}{3kd^2} = \frac{2R\left(f_0\left[w_R(uR)-w_L(uR)\right]-F(uR)\right)}{3kd^2}.$$

For round myofibril, Eq. 10 reduces to

$$\varsigma(u)\frac{\partial u}{\partial t} = \frac{\partial^2 u}{\partial r^2}\left(1+\mu\left(\frac{\partial u}{\partial r}\right)^2\right) + \frac{1}{r}\frac{\partial u}{\partial r}\left(1+\frac{\mu}{3}\left(\frac{\partial u}{\partial r}\right)^2\right)+\varphi(u) \tag{13}$$

and the boundary condition Eq. 11 give

$$\partial u/\partial r = 0 \quad \text{at } r=0 \quad \text{and} \quad \alpha\cdot\partial u/\partial r + u = 0 \quad \text{at} \quad r=1. \tag{13'}$$

Condition at $r = 0$ provides continuous gradient of $u$ in the center of sarcomere. At $\alpha = 0$ the boundary of the M-band is fixed in the middle of sarcomere. The bond between the M-band and extra-sarcomere cytoskeleton becomes loose when $\alpha$ increases in and completely disappears when $\alpha \to \infty$.

## 4 Results

### 4.1 Sarcomere with unconstrained M-band is unstable

Firstly we consider the simplest case of a loose M-band that is not connected to extra-sarcomere structures. For our model this corresponds to $\alpha \to \infty$. In this case the M-band remains flat, the M-band force, $f_M$, is identically equal to zero and the behavior of the sarcomere is fully determined by function $\varphi(u)$ that describes the net force of cross-bridges and I-band titin segments. In this case Eq. 10 reduces to a simple ordinary differential equation of the 1-st order. Figure 3 shows the force unbalance, $\psi(u)$, as function of the thick filament displacement $u$ for two sarcomere lengths, 2.25 and 2.7 μm on the plateau and the descending limb of the length-force diagram, respectively. Equilibrium states of the system correspond to points where the net force $\psi(u) = 0$.

On the plateau the M-band position in the middle of sarcomere ($u = 0$) is stable (Fig. 3a). Two other equilibrium states (points B and B′ in Fig. 3a) just outside the plateau region are unstable, while two other equilibrium points (A and A′ in Fig. 3a) are stable again. This means that a small initial fluctuation of the M-band that remains between points B′ and B will decay with time. For such small fluctuations the sarcomere restores its symmetric configuration with $u = 0$. However for larger initial fluctuations, outside the B′B segment, the symmetric configuration of the M-band will not be restored and the M-band will move to point A′ or A depending on the direction of the initial fluctuation. In practice, the shift of the M-band from the middle of sarcomere is limited not only by titin and cross-bridges, but also by Z-disks. Their positions are shown by dotted lines in Fig. 3. For a short sarcomere length the thick filament will hit a Z-disk after a large (outside B′B interval) initial displacement before reaching stable asymmetric equilibrium point A or A′.

On the descending limb the symmetric state $u = 0$ is unstable both locally and globally. For any initial fluctuation the M-band will move to a stable equilibrium point A′ or A′ (Fig. 3b). The stability of the symmetric sarcomere configuration against small fluctuations is determined by the sign of value $K$:

$$K = \left.\frac{d\varphi(u)}{du}\right|_{u=0}$$

that is the slope of function $\varphi(u)$ in the middle of sarcomere ($u = 0$). Parameter $K$ is negative if titin force prevails over the cross-bridge force so that the resulting force tends to return the thick filament to the middle of the sarcomere. $K$ is positive if the cross-bridge force destabilizing the system prevails over titin force. As seen from Fig. 3 the position of the M-band in the middle of sarcomere is stable against small fluctuations if $K < 0$ and unstable if $K > 0$.

On the ascending limb the symmetric configuration with $u = 0$ is also instable because the effective overlap zone between properly oriented actin and myosin heads increases in one half of a thick filament and decreases in another half. If $u > 0$, i.e. if the filament is shifted to the right, $w_R$ increases while $w_L$ decreases and vice versa. As the result cross-bridge force pull the filament in the direction of its displacement. For short sarcomere length the titin force is much smaller than the cross-bridge force (Fig. 2). Therefore on the ascending

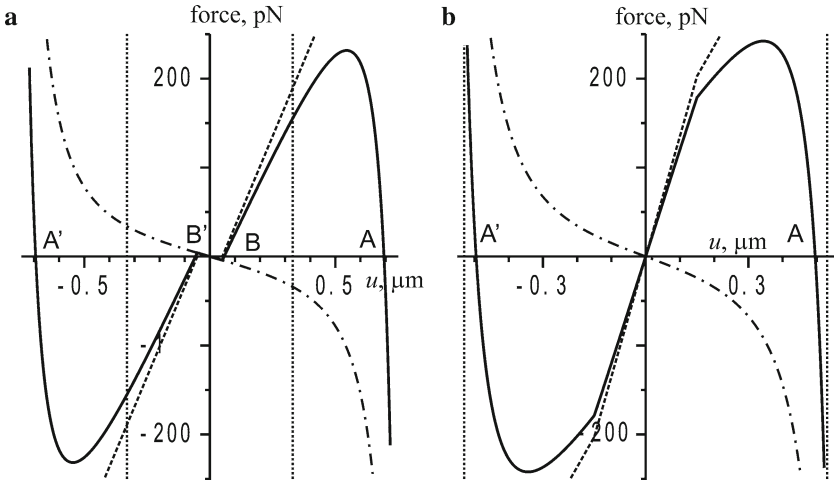


**Fig. 3** Analysis of stability of a sarcomere with unconstrained M-band. **a**, **b** Force plots at sarcomere length, $2l = 2.25$ and 2.7 μm, respectively. Titin force ($F(u)$, *dashed-dotted lines*), cross-bridge force, ($f_0[w_R(u) - w_L(u)]$, *dashed lines*), and their sum (*continuous lines*) per a thick filament are shown as the functions of the M-band displacement from the middle of sarcomere, $u$. Points A and A′ are the points of stable equilibrium of the system, B and B′ are unstable equilibrium points. The origin that corresponds to the symmetric sarcomere configuration is stable in case **a** and unstable in case **b**. *Vertical dotted lines* represent the positions where the tips of the thick filaments hit the Z-disks. In case **a** they limit the A-band movement towards equilibrium points A and A′. Model parameter values are in the text and in the notification table

limb a thick filament will move the whole way to the closest Z-disk after any small fluctuation.

### 4.2 M-band anchoring in extra-sarcomere cytoskeleton increases stability

Now we consider how anchoring of the M-band in extra-sarcomere cytoskeleton structures affects stability of symmetric configuration of a sarcomere. For small M-band fluctuations from the middle of a sarcomere all nonlinear terms can be omitted so that Eq. 12 for thin rectangular myofibril can be rewritten as

$$\varsigma(0)\,\frac{\partial u}{\partial t} = \frac{\partial^2 u}{\partial x^2} + Ku. \tag{14}$$

General solution of Eq. 14 can be obtained using the Fourier method. It gives

$$u(x,t) = \sum_{n=1}^{\infty} u_n^0 \exp(-\lambda_n \varsigma(0)\,t)\cos\left(x\sqrt{\lambda_n \eta\,(0) + K}\right)$$

where $u_n^0$ is the initial fluctuation of the $n$th mode and $\lambda_n$ is $n$th root of the equation

$$-\alpha\sqrt{\lambda\varsigma(0)+K}\cdot\sin\sqrt{\lambda\eta\,(0)+K} + \cos\sqrt{\lambda\varsigma(0)+K} = 0$$

that results from the boundary condition at $x = 1$ (Eq. 12'). The stability of the trivial symmetric solution ($u \equiv 0$) against any small initial fluctuation is provided if all fluctuations decay with time. As $\zeta(0) > 0$, this means that $\lambda_n > 0$ for all $n$. For fixed M-band boundary($\alpha = 0$) this condition is satisfied when $K < K_{\text{crit}} = \pi^2/4 \approx 2.47$. For $\alpha > 0$, $K_{\text{crit}}$ decreases to zero when $\alpha$ increases approaching infinity and approaches zero at $\alpha \to \infty$ (Fig. 4a).

Similarly, Eq. 13 for small M-band displacements in a round myofibril reduces to

$$\eta(0)\,\frac{\partial u}{\partial t} = \frac{\partial^2 u}{\partial r^2} + \frac{1}{r}\frac{\partial u}{\partial r} + Ku. \tag{15}$$

Its trivial solution $u \equiv 0$ is stable against any small fluctuation if all roots $\lambda_n$ of the equation

$$\alpha\sqrt{\lambda_n\varsigma(0)+K}\,\frac{dJ_0(r)}{dr}\bigg|_{r=\sqrt{\lambda_n+K}} + J_0\left(\sqrt{\lambda_n\varsigma(0)+K}\right) = 0$$

are positive. Here $J_0(x)$ is the 0th order Bessel function of the first kind. For $\alpha = 0$ the stability condition is reduced to $K \le K_{\text{crit}} = \mu_1^2$ where $\mu_1 \approx 2.405$ is the 1-st root of $J_0(x)$ so that $K_{\text{crit}} \approx 5.78$. Figure 4b shows how $K_{\text{crit}}$ decreases with increase in $\alpha$ for round sarcomere. For any given $\alpha$ round myofibril is more stable that the thin rectangular one with the same size $R$ and model parameters (Fig. 4).

It is worth mentioning that more general two-dimensional M-band fluctuations in a round or thin rectangular sarcomere are more stable that the one-dimensional fluctuations considered above.

The linear analysis shows that the M-band stiffness and the presence of a stiff bond between the M-band border and extra-sarcomere structures increase the stability of the symmetric configuration of a sarcomere. There is a safe range of positive $K$ values where sarcomere remains stable and the M-band keeps its flat shape despite cross-bridge forces

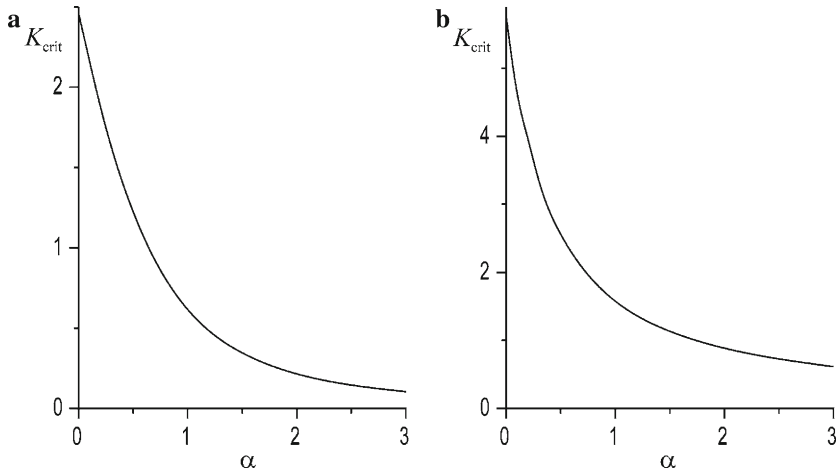


**Fig. 4** The dependence of the critical $K$ value, $K_{crit}$, on the dimensionless boundary stiffness parameter, $\alpha$, for the thin rectangular (**a**) and round (**b**) sarcomeres. $K$ is the slope of the net cross-bridge/titin force that destabilizes the central position of the M-band (negative stiffness) normalized for the M-band stiffness

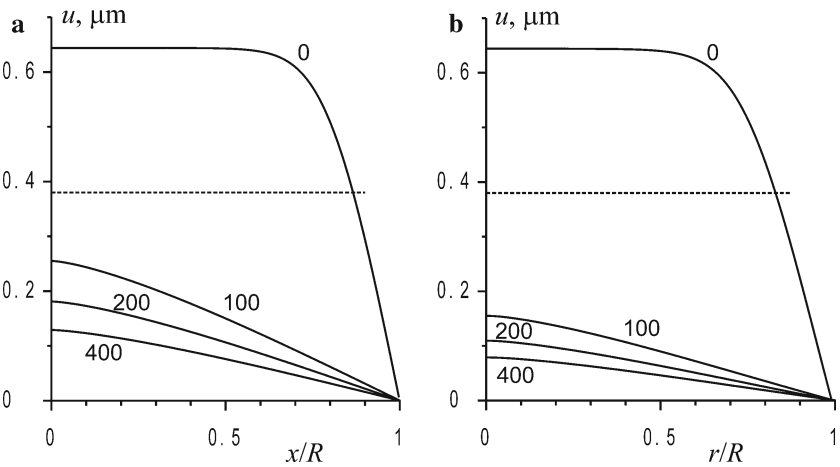


**Fig. 5** The calculated buckled shape of the M-band for thin rectangular (**a**) and round (**b**) sarcomere. Dimensional displacement, $u$, is shown as a function of dimensionless coordinate from the center of the sarcomere, $x/R$ or $r/R$. *Horizontal dashed lines* show the distance between the tip of the thick filament and the Z-disk. Figures next to the plots are the values of the dimensionless non-linearity parameter, $\mu$; $l = 1.2$ μm, $k = 2$ pN/nm, other parameters are specified in the text

trying to destabilize the system. The loss of stability occurs only when $K$ exceeds $K_{crit}$. When this happens, the symmetric configuration of sarcomere cannot be maintained and the M-band buckles.

### 4.3 Buckled shape of the M-band, effect of non-linearity of its elasticity

Linear model predicts unrealistic unrestricted buckling at super-critical $K$ values. Therefore nonlinear terms should be taken into account to simulate the buckled shape of the M-band under super-critical force. For this, steady state solutions of the ordinary differential equations obtained from Eqs. 12 and 13 by setting $v = \partial u/\partial t \equiv 0$ were solved numerically with boundary conditions Eqs. 12' and 13', respectively. Although Eq. 12 can be solved in quadratures, in practical terms it was easier to use a forth-order Runge–Kutta method for both boundary problems. Value of $u(0)$ in the center of the sarcomere was selected using an iterative procedure (shooting) to match the second boundary conditions at $x = 1$ or $r = 1$ with the accuracy of $10^{-4}$.

Figure 5 shows calculated buckled shapes of the M-band when its boundary is fixed in the middle of sarcomere, $\alpha = 0$, at the end of the plateau of the length tension diagram ($l = 1.2$ μm) for different values of the M-band non-linearity parameter, $\mu$. If the M-bond elasticity is linear ($\mu = 0$) the buckling amplitude, $u_{max}$, is limited only by non-linearity of the titin elasticity. In this case $u_{max}$ is determined by the contour length of the I-band titin segment, $L_c$, and is practically independent of the M-band stiffness, $k$,irrespectively on the cross-section shape of the sarcomere (Fig. 5a, b). The $u_{max}$ value calculated for $\mu = 0$ is unrealistically high, ca. 640 nm ($\approx 1.3R$ at $R = 500$ nm), that is larger than the distance between the tip of the thin filaments and a Z-disk (Fig. 5). To obtain a reasonable buckled shape with $u_{max}$ of 0.1–0.2 dimensionless unit one should set the dimensionless non-linearity parameter, $\mu$, to a high value of 200–400 (Fig. 5). In this case the steady-state distributions $u(x)$ and $u(r)$ for both thin rectangular and round sarcomeres are close to parabola (Fig. 5a, b).

An increase in maximal isometric cross-bridge force $F_0 = f_0(l_m - l_b)$ leads to an increase in the buckling amplitude

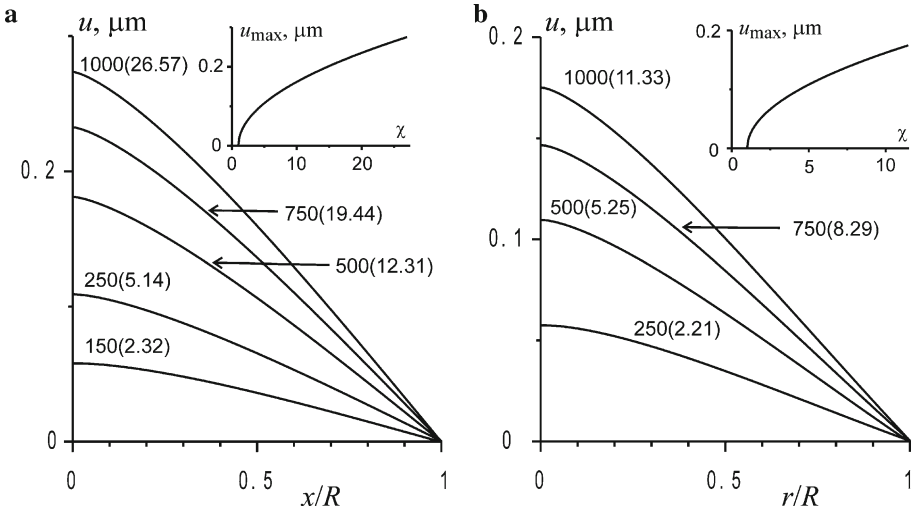


**Fig. 6** The calculated buckled shape of the M-band for rectangular (**a**) and round (**b**) sarcomere as a function of the cross-bridge force per half thick filament at full overlap (cross-bridge forces pulling each half of a thick filament $F_0$ are shown in pN next to curves, the supercriticality parameter $\chi = K/K_{\text{crit}}$ for each force value is shown in brackets). Insets show calculated dependence of the dimensional buckling amplitude $u_{\max}$ (μm) on $\chi$ for rectangular and round sarcomere, respectively; dimensionless non-linearity parameter $\mu = 200$; all other parameters are as in Fig. 5

$u_{\max}$. The dependence of $u_{\max}$ on $F_0$ is very steep when the supercriticality parameter $\chi = K/K_{\text{crit}}$ only slightly exceeds 1 and flattens at high $F_0$ and $\chi$ (Fig. 6). The dependence of the dimensionless buckling amplitude $u_{\max}$ on $\chi$ for $\mu = 200$ can be well fitted with formula: $u_{\max} = A\sqrt{\chi - 1}$ where $A \approx 0.108$ for both round and thin rectangular myofibril.

Increase in $\alpha$, i.e. softening of the bond between the M-band border and extra-sarcomere cytoskeleton induces sliding of the M-band border with respect to the middle of sarcomere after its buckling and to a more pronounced buckling due to increased unbalance of the cross-bridge forces pulling the thick filaments towards the left and right Z-disks. The shape of the M-band becomes in this case non-parabolic with a rather sharp tip in the center of the sarcomere and near linear gradient in the outer part of the sarcomere (Fig. 7). The non-linearity of the M-band elasticity can effectively keep the buckling amplitude within reasonable range even if the M-band anchoring in the extra-sarcomere cytoskeleton is not absolutely stiffly (Fig. 7).

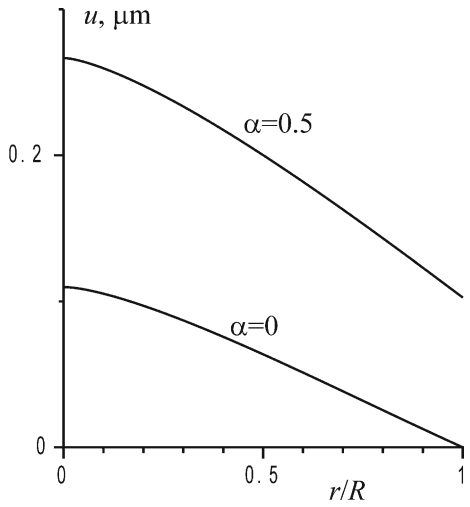


**Fig. 7** Calculated buckled shape of the M-band for round sarcomere at $\alpha = 0$ (stiff M-band anchoring) and $\alpha = 0.5$ (elastic M-band anchoring); dimensionless non-linearity parameter $\mu = 200$. Cross-bridge force per half-thick filament at full overlap $F_0 = 500$ pN; all other parameters are as in Figs. 3, 5

### 4.4 The time course of the M-band buckling

To simulate the loss of stability of the symmetric shape of the sarcomere after a small fluctuation, non-linear non-steady equations (12), (12') or (13), (13') were solved numerically using an implicit solver. A small ($\leq 10^{-3}$ in dimensionless $u$ units) bell-shaped fluctuation that satisfies the boundary conditions was introduced as initial condition at $t = 0$. Examples of calculation with $\alpha = 0$ and $\alpha = 0.5$ at $l = 1.2$ μm are shown in Fig. 8. The M-band deviation from the middle of the sarcomere is maximal in the center of sarcomere. The time course of buckling is S-shaped; the smaller initial fluctuation the later the buckling begins. The dimensionless rise time from 10 to 90% of the full buckling amplitude is 0.1–0.13 dimensionless time units (Fig. 8) independently on the size of initial fluctuation.

## 5 Discussion

The M-band has been assumed to be a "safeguard of sarcomere stability" (Agarkova et al. 2003). More recently shear

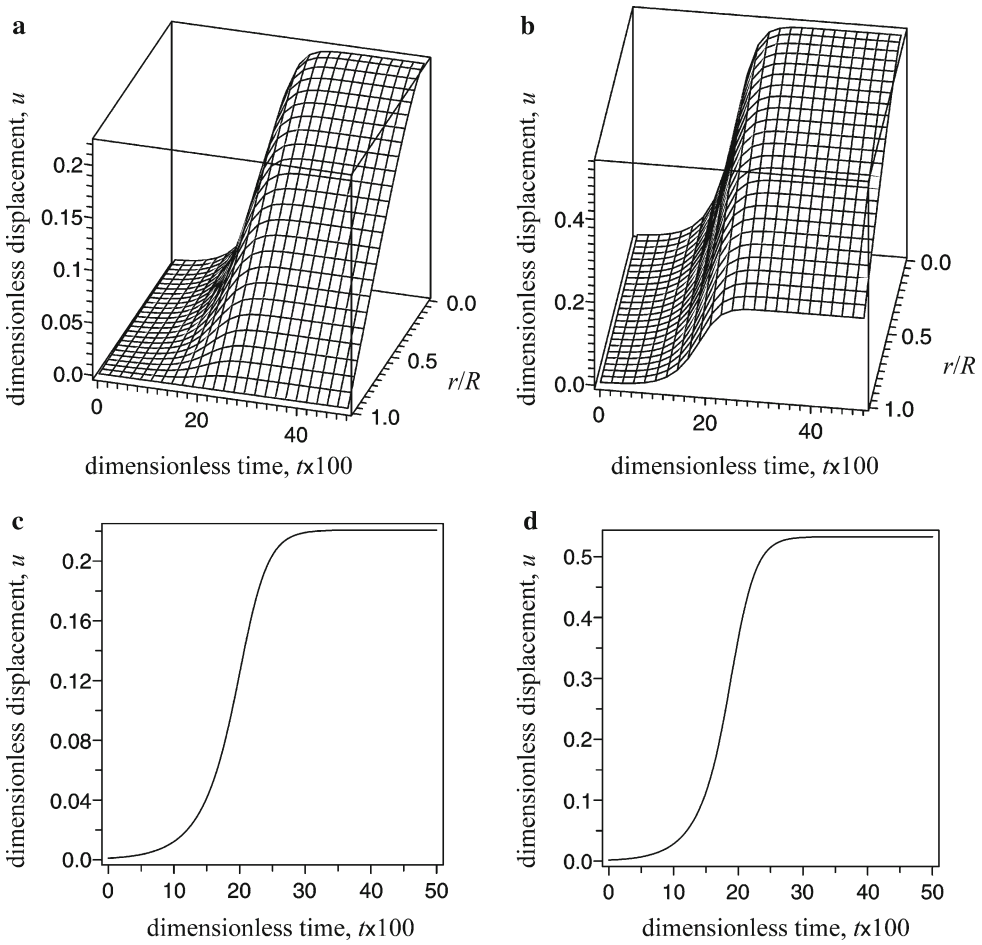


**Fig. 8** Calculated time course of the M-band buckling for round myofibril. **a**, **c** $\alpha = 0$; **b**, **d** $\alpha = 0.5$. **a**, **b** The two-dimensional plots of the dimensionless displacement, $u(x, t)$ or $u(r, t)$; **c**, **d** the time course of the displacement in the center of the sarcomere (at $r = 0$ or $x = 0$) where the thick filament displacement is maximal. Same parameter values as in Fig. 7

strain of the M-band was suggested to underlie mechanosensing of TK (Puchner et al. 2008). However it remained unclear how the M-band stabilizes a sarcomere and what mechanical factors induce its shear stress that activates TK. Here we present a mechanistic model of sarcomere that explains how and why the M-band may keep the thick filaments in the center of sarcomere when myosin cross-bridges produce high force. It also explains how and why the force may induce shear strain in the M-band that triggers the TK signaling.

### 5.1 Comparison with experimental observations, estimation of model parameters

The modeling results suggest that the M-band should buckle when active sarcomere tension exceeds a certain critical limit. Experimentally the buckling can be observed in the x-ray diffraction pattern as widening of the M3 myosin meridional reflection upon development of active tension (Huxley et al. 1982). The M3 reflection arises from crowns of myosin heads projecting from the backbone of the thick filament every ca. 14.5 nm. When all thick filaments are aligned in the middle of sarcomere and the M-band is flat, all crowns of myosin heads scatter X-rays coherently and the M3 reflection is very narrow. Its width in the equatorial direction corresponds to a coherently scattering structure of ~1 μm diameter that is close to sarcomere width (Huxley and Brown 1967). Upon activation the M3 reflection widens in parallel with tension development due to misalignment of the thick filaments (Huxley et al. 1982; Brunello et al. 2006). We suggest that the filament misalignment and the M3 widening are caused by the loss of the M-band stability and its buckling considered here. The widening of the M3 reflection occurs when tension achieves 10–20% of its maximal isometric value (Huxley et al. 1982; Griffiths et al. 2006). This means that on plateau of isometric tetanus at full filament overlap the supercriticality parameter, $\chi = K/K_{\text{crit}}$, is between 5 and 10. Quantitative estimate of the root mean squared shear strain during isometric contraction can be obtained by fitting experimental M3 profile with a model of X-ray diffraction that takes into account filament axial disorder of the second kind (Koubassova and Tsaturyan 2002; Koubassova et al. 2008). This approach gives an estimate of the root mean squared shear strain of

3.5–5.5 nm per ~40 nm distance, $d$, between neighbor thick filaments that correspond to ~0.1 in dimensionless $\nabla u$ units during isometric contraction of maximal amplitude. Increase in isometric tension developed by muscle fibers by a factor of 1.44 upon increase in temperature from 0°C to 17°C in intact frog muscle fibers is accompanied by widening of the M3 reflection by only 16% (Linari et al. 2005). This agrees with results of our modeling showing only small increase in the amplitude of the M-band buckling with force much higher than critical (Fig. 6). Using reasonable parameters of titin elasticity ($L_p = 1.2$ nm, $L_c = 1150$ nm, Leake et al. 2004), maximal cross-bridge force per a thick filament $F_0 = f_0(l_m - l_b) = 500$ pN (that corresponds to 1.6 pN per myosin head) and sarcomere width $R = 0.5$ μm one can estimate stiffness of the M-band bond between the adjacent thick filaments, $k$, that provides a reasonable value of the supercriticality parameter. For inter-filament stiffness $k$ of 2 pN/nm that is higher than stiffness of the TK domain (<1 pN/nm, Puchner et al. 2008) and the softest EH-domain of myomesin (~1 pN/nm, Schoenauer et al. 2005) we have $\chi = 12.3$ for thin rectangular and $\chi = 5.25$ for round myofibril, respectively. The detailed structure of the M-band is unknown so that we do not know what amount of strain is induced in each M-band protein when a thick filament moves by a certain distance along its axis with respect to the adjacent filaments. Stoichiometry suggests that the connection between two adjacent thick filaments contains the M-band region of two titin molecules (Liversage et al. 2001), probably several pairs of myomesin molecules (Agarkova and Perriard 2005) and perhaps some other proteins. In any case our estimate of the M-band bending stiffness seems to be of reasonable value compared to the results of direct measurements of the TK and myomesin elasticity. It is worth mentioning that an increase or decrease of $k$ by a factor of two would only marginally affect the results of the analysis presented here as at high supercriticality the buckling amplitude is mainly determined by the nonlinearity of elastic properties of the M-band.

As revealed by our modeling, the M-band stiffness can effectively increase stability of the symmetric configuration of sarcomere and limit the amplitude of its buckling under supercritical force only if the boundary of the M-band is anchored in the extra-sarcomere cytoskeleton. In terms of our model this means that dimensionless parameter $\alpha$ should be 0.5 or less. In dimensional variables this corresponds to $E \geq \sqrt{3}kd/R \approx 0.28$ pN/nm if $k = 2$ pN/nm, $d = 40$ nm and $R = 500$ nm. Such stiffness is of reasonable value for long multi-domain structural proteins such as titin and myomesin. The stiffness of the extra-sarcomere cytoskeleton estimated is small enough to be a minor contributor to the total passive sarcomere stiffness compared to titin (Granzier and Irving 1995).

Our modeling suggests that at high supercriticality that is characteristic for maximal contracting force ($\chi \approx 5$–10) the amplitude of the M-band buckling should be unrealistically high if the M-band elasticity is linear (Fig. 5). Substantial non-linearity of the M-band elasticity limits the buckling amplitude (Fig. 5) even if the connection between the M-band and extra-sarcomere cytoskeleton in not very stiff (Fig. 7). Such limitation is useful for protection of sarcomeres from damage and for sustaining optimal muscle performance at high, super-critical force. Reasonable limitation of the buckling amplitude can be achieved with the dimensionless nonlinearity parameter $\mu$ between 200 and 400. In dimensional terms this means that the tangent axial stiffness of the connection between two neighbor thick filaments doubles when relative filament displacement increases from zero to 3–4.2 nm. Such nonlinearity is close to its value found for a single TK domain using atomic force microscopy (Puchner et al. 2008).

Modeling also suggests that weakening or damage of the bond between the M-band and extra-sarcomere structures ($\alpha \to \infty$) should eliminate the role of the M-band in the stability of symmetric sarcomere configuration (Figs. 3, 4) and diminish the M-band shear strain under force development. This agrees with the experiments with single isolated myofibrils where tension development was accompanied by a significant shift of the M-bands towards one of the Z-disks without a significant bending of the M-bands (Telley et al. 2006).

### 5.2 Limitations of the model

Although our modeling was performed only for the simplest case of a single sarcomere with fixed length, we believe that the main conclusions concerning the stability of the symmetric configuration of a sarcomere and the dependence of the buckled shape on the main model parameters are relevant for a more complex and more realistic case of a number of sarcomeres connected in series. The Z-disks are also not absolutely stiff and may bend under certain conditions. Neighbor myofibrils are connected to each other across the fiber in the regions of the Z-disks and M-bands. Therefore some shear strain may occur on the level of whole fiber. Modeling that takes into account these effects may be a subject of future studies.

Another limitation of the model is that mechanical properties of the cross-bridges are described by the simplest linearized Hill model that cannot account for high dynamic stiffness and fast partial tension recovery after step length changes (Huxley–Simmons phases 1 and 2) which determine mechanical properties of cross-bridges on the time scale of several ms or faster. In the present form the model can only describe quasi-steady-state cross-bridge properties and to simulate contraction kinetics on the time scale of tens of ms or slower. In dimensional terms the buckling time for examples

shown in Fig. 8 corresponds to 0.5–1 s. On the other hand fast tension transients in attached cross-bridges can themselves cause sarcomere instability (Vilfan and Duke 2003). More detailed cross-bridge model that takes into account dynamic equilibrium of attaches cross-bridge states can in principle be incorporated into the model considered here. However this will unavoidably complicate the analysis.

### 5.3 Proposed role of the M-band buckling in TK mechano-sensing

Although titin kinase is believed to be the sensor that triggers mechanical control of gene expression and protein turnover in muscle (Lange et al. 2005; Puchner et al. 2008) it was unclear how TK may sense strain or stress being localized in the M-band. Our modeling suggests a plausible explanation of the mechanism of TK mechano-sensing. In relaxed muscle or at low active tension, sarcomere remains stable, the M-band is flat and TK is unstrained. Under these conditions the TK activity is inhibited because its ATP-binding center is blocked by the TK regulatory tail (Puchner et al. 2008). When the M-band buckles at super-critical active force, a shear strain appears in the M-band. It stretches TK, opens its ATP binding center and launches the mechano-signaling cascade as suggested by Puchner et al. (2008). Such buckling-induced mechanism suggests some specific features of the TK mechano-sensing which may be of biological importance. Firstly, no shear strain in the M-band and no TK stretch occur until active force reaches its critical level. This sets a threshold for the TK response to mechanical load preventing unnecessary energy consumption for gene expression and protein synthesis. On the other hand when the cross-bridge force is too high the buckling amplitude remains moderate if the M-band elasticity is nonlinear (Fig. 6) thus protecting sarcomere integrity.

**Acknowledgments** The work was supported by grants from the Russian Foundation for Basic Research and from the Grant Committee of the President of Russian Federation.

## References

Agarkova I, Ehler E, Lange S, Schoenauer R, Perriard JC (2003) M-band: a safeguard for sarcomere stability? J Muscle Res Cell Motil 24:191–203

Agarkova I, Perriard JC (2005) The M-band: an elastic web that cross-links thick filaments in the center of the sarcomere. Trends Cell Biol 15:477–485

Brunello E, Bianco P, Piazzesi G et al (2006) Structural changes in the myosin filament and cross-bridges during active force development in single intact frog muscle fibres: stiffness and X-ray diffraction measurements. J Physiol 577:971–984

Carlsson L, Yu JG, Thornell LG (2008) New aspects of obscurin in human striated muscles. Histochem Cell Biol 130:91–103

Cunha SR, Mohler PJ (2008) Obscurin targets ankyrin-B and protein phosphatase 2A to the cardiac M-line. J Biol Chem 283:31968–31980

Fukuzawa A, Lange S, Holt M et al (2008) Interactions with titin and myomesin target obscurin and obscurin-like 1 to the M-band: implications for hereditary myopathies. J Cell Sci 121:1841–1851

Granzier HL, Irving TC (1995) Passive tension in cardiac muscle: contribution of collagen, titin, microtubules, and intermediate filaments. Biophys J 68:1027–1044

Griffiths PJ, Bagni MA, Colombini B, Amenitsch H, Bernstorff S, Funari S, Ashley CC, Cecchi G. (2006) Effects of the number of actin-bound S1 and axial force on X-ray patterns of intact skeletal muscle. Biophys J 90:975–984

Grove BK, Kurer V, Lehner C et al (1984) A new 185,000-dalton skeletal muscle protein detected by monoclonal antibodies. J Cell Biol 98:518–524

Hill AV (1953) The mechanics of active muscle. Proc R Soc Lond B 141:104–117

Hornemann T, Kempa S, Himmel M, Hayess K, Fürst DO, Wallimann T (2003) Muscle-type creatine kinase interacts with central domains of the M-band proteins myomesin and M-protein. J Mol Biol 332:877–887

Horowits R, Podolsky RJ (1987) The positional stability of thick filaments in activated skeletal muscle depends on sarcomere length: evidence for the role of titin filaments. J Cell Biol 105:2217–2223

Huxley HE, Brown W (1967) The low-angle X-ray diagram of vertebrate striated muscle and its behaviour during contraction and rigor. J Mol Biol 30:383–434

Huxley HE, Faruqi AR, Kress M et al (1982) Time-resolved X-ray diffraction studies of the myosin layer-line reflections during muscle contraction. J Mol Biol 158:637–684

Huxley HE, Stewart A, Sosa H, Irving T (1994) X-ray diffraction measurements of the extensibility of actin and myosin filaments in contracting muscle. Biophys J 67:2411–2421

Koubassova NA, Tsaturyan AK (2002) Direct modeling of X-ray diffraction pattern from skeletal muscle in rigor. Biophys J 83:1082–1097

Koubassova NA, Bershitsky SY, Ferenczi MA, Tsaturyan AK (2008) Direct modeling of X-ray diffraction pattern from contracting skeletal muscle. Biophys J 95:2880–2894

Lange S, Xiang F, Yakovenko A et al (2005) The kinase domain of titin controls muscle gene expression and protein turnover. Science 308:1599–1603

Leake MC, Wilson D, Gautel M, Simmons RM (2004) The elasticity of single titin molecules using a two-bead optical tweezers assay. Biophys J 87:1112–1135

Linari M, Brunello E, Reconditi M et al (2005) The structural basis of the increase in isometric force production with temperature in frog skeletal muscle. J Physiol 567:459–469

Liversage AD, Holmes D, Knight PJ et al (2001) Titin and the sarcomere symmetry paradox. J Mol Biol 305:401–409

Luther P, Squire J (1978) Three-dimensional structure of the vertebrate muscle M-region. J Mol Biol 125:313–324

Obermann WM, Gautel M, Steiner F et al (1996) The structure of the sarcomeric M band: localization of defined domains of myomesin, M-protein, and the 250-kD carboxy-terminal region of titin by immunoelectron microscopy. J Cell Biol 134:1441–1453

Puchner EM, Alexandrovich A, Kho AL (2008) Mechanoenzymatics of titin kinase. Proc Natl Acad Sci USA 105:13385–13390

Schoenauer R, Bertoncini P, Machaidze G et al (2005) Myomesin is a molecular spring with adaptable elasticity. J Mol Biol 349:367–379

Schoenauer R, Lange S, Hirschy A et al (2008) Myomesin 3, a novel structural component of the M-band in striated muscle. J Mol Biol 376:338–351

Sosa H, Popp D, Ouyang G, Huxley HE (1994) Ultrastructure of skeletal muscle fibers studied by a plunge quick freezing method: myofilament lengths. Biophys J 67:283–292

Telley IA, Denoth J, Stüssi E et al (2006) Half-sarcomere dynamics in myofibrils during activation and relaxation studied by tracking fluorescent markers. Biophys J 90:514–530

Tsaturyan AK, Koubassova N, Ferenczi MA et al (2005) Strong binding of myosin heads stretches and twists the actin helix. Biophys J 88:1902–1910

Trombitás K, Tigyi-Sebes A (1984) Cross-bridge interaction with oppositely polarized actin filaments in double-overlap zones of insect flight muscle. Nature 309(5964):168–170

Vilfan A, Duke T (2003) Instabilities in the transient response of muscle. Biophys J 85:818–827

Wakabayashi K, Sugimoto Y, Tanaka H et al (1994) X-ray diffraction evidence for the extensibility of actin and myosin filaments during muscle contraction. Biophys J 67:2422–2435

Zahalak GI (1997) Can muscle fibers be stable on the descending limbs of their sarcomere length-tension relations? J Biomech 30:1179–1182